

# Liquid-like H<sub>2</sub>O adsorption layers to catalyze the Ca(OH)<sub>2</sub>/CO<sub>2</sub> solid–gas reaction and to form a non-protective solid product layer at 20°C

Dario T. Beruto\*, Rodolfo Botter

*Dipartimento di Edilizia, Urbanistica e Ingegneria dei Materiali (DEUIM), Università di Genova, 16126 Genova, Italy*

Received 17 February 1999; received in revised form 14 June 1999; accepted 3 July 1999

## Abstract

Porous calcium hydroxide particles have been equilibrated with water vapor in the relative pressure range 0.4–0.85 at the temperature of 20°C. Then the particles were used in the reaction with gaseous carbon dioxide at the same temperature and at pressure of 0.65 kPa. The system is converted up to 85% into a non-protective layer of calcium carbonate which is all distributed inside the initial porous particles. The same reaction with dry-calcium hydroxide powders converts up to 10% at a temperature of 100°C. The observed catalytic effect is dependent upon the initial amount of water adsorbed. A minimum number of four layers of water adsorbed onto the calcium hydroxide surfaces is required to promote the catalytic effect. © 2000 Elsevier Science Ltd. All rights reserved.

*Keywords:* Ca(OH)<sub>2</sub>; Catalysis; CO<sub>2</sub>; Porosity; Powders-gas phase reaction

## 1. Introduction

Many important reactions between gases, like SO<sub>2</sub>, SO<sub>3</sub><sup>1</sup> and CO<sub>2</sub>,<sup>2</sup> and solids such as calcium carbonates and calcium hydroxides, can use dry solid powders and/or solid powders dispersed in aqueous media. Important technological advantages and disadvantages are related to these processing conditions. Usually the gas–solid processes require a high reaction temperature due to the fact that interfacial reactions, followed by solid-state diffusion steps, are the rate controlling steps. The solid reaction products can form a protective layer around the reacting particles, so that conversion can be hardly complete. Nevertheless, in comparison with the similar processes that use the aqueous solid particles dispersions as reaction medium, this technology handles less volume of matter and the further manipulations of the reaction products are easy to do. On the other hand, the reactions occurring in the liquid phase environment are characterized by the partial dissolution of the solid reactants followed by the precipitation of a new solid

phase. Because of these features the new solid reaction products do not form a protective layer, so that the reaction can reach a high degree of conversion at reduced reaction temperatures.<sup>3</sup>

For the purpose of combining the advantages of the gas–solid process and that of the liquid–solid–gas ones, in this paper we will deal with the reaction between CO<sub>2</sub> (g) and solid porous particles of Ca(OH)<sub>2</sub>. This process can be usually considered as a classical gas–solid reaction. However, if the starting reacting calcium hydroxides powders are covered with a H<sub>2</sub>O (v) multilayer adsorbed film, there is a hope of transforming this reaction into a liquid–solid–gas process. In fact, the adsorbed multilayer regions form a bidimensional (2D) liquid-like interface,<sup>4</sup> where Ca<sup>2+</sup> and OH<sup>−</sup> ions can be formed as a consequence of the solubility of the calcium hydroxide surfaces in the liquid-like nanometric adsorbed phase. Thus the carbonation reaction could proceed through the reaction between these ions and the gaseous carbon dioxide, only the amount of water vapor adsorbed is stable all along the progress of the carbonation reaction. This is no easy task to perform.

To test whether or not this possibility is feasible is the first goal of this paper. To obtain the most important chemical reactions controlling the new process and to

\* Corresponding author. Tel.: +39-10-353-6039; fax: +39-10-353-6036.

*E-mail address:* dabe@unige.it (D.T. Beruto).

evaluate the microstructure evolution occurring within the reacting porous particles are the other important issues of this experimental study.

Evidence that a mixture of powders obtained by high temperature limestone injection in a boiler can, when treated with water vapor near 100°C, further react with sulfur oxides near that temperature at high water vapor pressure has been given by Staudinger and co-workers.<sup>5</sup>

The powder systems and the experimental conditions used in Staudinger's pilot plant are such that it is difficult to establish the role of the adsorbed water vapor on that sulfur-removal process. Nevertheless the possibility of using a 2D solution chemistry to modify a complex gas–solid phenomenon could be usefully adopted also in removal of SO<sub>2</sub> and SO<sub>3</sub> gas from combustion products.<sup>6</sup>

## 2. Experimental

### 2.1. Materials

Reagent grade calcium hydroxide powders have been used throughout this work. The powders were formed by porous grains of irregular shape characterized by several levels of microstructure, SEM, XRD and N<sub>2</sub>-adsorption techniques at –195°C were used to investigate the microstructure at the different levels.

To obtain reliable adsorption data it is important that the surface area of the particles as well as their porosity does not change during the adsorption test. It has been demonstrated<sup>7</sup> that a pre-treatment of the powders with the same adsorbent gas can stabilize the solid microstructure. Consequently the samples were pre-treated in water vapor at 25°C and at a partial pressure of 3 kPa for 72 h. The initial surface area of the particles decreased from 9 to 6 m<sup>2</sup>/g. This last value has turned out to be stable when the hydroxide particles were exposed subsequently to different relative partial pressures of water vapor at the same temperature.

### 2.2. Techniques

300 mg of Ca(OH)<sub>2</sub> were placed in a Pt crucible inside a symmetrical thermobalance already described elsewhere.<sup>8</sup> The system was evacuated at the temperature of 110°C using a diffusion pump for about 2 h. Then the temperature was lowered to 20°C and water vapor, from a connected line, was admitted, at the same temperature, into the system at different and pre-selected values of relative humidity (RH). The relative partial pressure range between 0.4 and 0.9 was explored. For each pre-selected water vapor partial pressure the temperature of the system was kept constant at 20°C ± 0.1 using a water jacket as controlling system. The mass of the gas inside the system is much larger than the one adsorbed by the specimen, so that the adsorption step

does not practically affect the total pressure of the gas into the chamber. Under this assumption, the water adsorption measurements were made at constant temperature and pressure. The sample weight was continuously recorded up to a steady-state value that was reached in about 30 min.

To test whether these steady-state adsorption values approach or not the thermodynamic ones, occasionally, when the steady adsorption state was reached, at constant temperature, the water vapor pressure was reduced and then raised again to the previous value. Initially the sample weight was observed to decrease with the vapor pressure. Then it moved back to the initial value when the pressure value was restored. Accordingly, the derived-adsorption data should be very near the thermodynamic equilibrium states.

When the sample was equilibrated with water vapor, a fixed amount of carbon dioxide was admitted into the chamber, leaving the temperature unchanged and keeping the external relative humidity at the same initial value. The changes in sample weight were continuously recorded with a sensitivity of 5 × 10<sup>–4</sup> mg/min. N<sub>2</sub> (g) was admitted into the system at the end of the process and the sample was taken off and split in different parts for further analysis.

To test the influence of the water vapor partial pressure and that of the carbon dioxide partial pressure on the carbonation process, this procedure was repeated for different values of the gas/vapor pressures.

To evaluate the total degree of carbonation, a portion of the treated sample was heated up to 950°C in air into another thermobalance. Other samples portions were used for SEM, XRD observations and for mercury porosimeter analysis.<sup>9</sup> When pore size analysis in the range of N<sub>2</sub>-adsorption isotherms was requested the samples were placed again in the symmetrical thermobalance and N<sub>2</sub>-adsorption desorption isotherms were taken at –195°C.<sup>10</sup>

H<sub>2</sub>O (v) adsorption isotherms at the temperature of 20°C were taken on Ca(OH)<sub>2</sub> and on CaCO<sub>3</sub> powder samples to evaluate their different adsorption capacities, with respect to water, at the same values of temperature and relative water vapor pressure.

## 3. Results and discussions

Fig. 1 illustrates the macroscopic structure of the initial calcium hydroxide powders. The particles are characterized by an irregular block-like shape with a linear dimension ranging between 10 and 50 μm. Each particle is a porous cluster of small grains. SEM observations at higher magnification (× 50 000) allow to characterize the average size of individual grains ranging between 0.5 and 2 μm. The grains have an irregular shape, probably more extended along the planar direction.

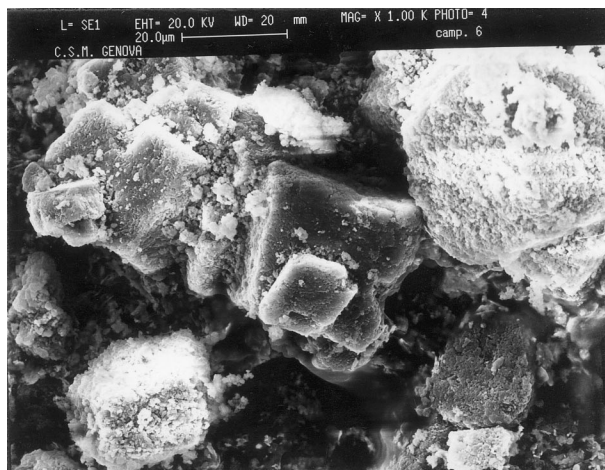


Fig. 1. Structure of the starting  $\text{Ca}(\text{OH})_2$  powders.

Fig. 2 shows the cumulative volume of mercury intruded into the powder bed — curve A — and the pore size distribution derived from these data<sup>11</sup> — curve B. It can be observed that the amount of mercury initially intruded corresponds to cavities larger than particle size. Accordingly these voids cannot be ascribed to internal particle pores but are due to pores within the powder bed. The fraction of porosity that can be due to internal particles porosity is clustered around an average size of  $1.5 \mu\text{m}$  in diameter, close to the average size of the individual grain. The corresponding porosity amounts to about  $0.3 \text{ cm}^3/\text{g}$ .

Fig. 3 shows the typical adsorption — desorption isotherms for  $\text{Ca}(\text{OH})_2$  powders obtained using  $\text{N}_2$  as adsorbent at  $-195^\circ\text{C}$ . According to Brunauer's classification,<sup>12</sup> these isotherms are II type isotherms. This result is peculiar to calcium hydroxide and calcium oxide powders derived from their thermal decomposition in vacuum.<sup>13</sup> The area of the hysteresis loop between the adsorption and the desorption isotherms is almost negligible, thus the contribution of the mesoporosity,<sup>14</sup> i.e. pores with average size less than  $50 \text{ nm}$ , is almost negligible in comparison with the porosity due to the larger cavities. Application of the  $t$ -method,<sup>15</sup> in the relative partial pressure range included between  $0.1$  and  $0.4$ , allows to exclude the presence of microporosity (pore size less than  $1 \text{ nm}$ ) and yields a surface area of  $6 \text{ m}^2/\text{g}$  in quite good agreement with the BET calculations.<sup>16</sup>

From all such information the microstructure of the starting powders can be envisaged as formed by two interconnected and disordered networks, where grains and pores have almost the same average cross-dimension equal to about  $1.5 \mu\text{m}$ . The obtained microstructure does not change for subsequent water vapor treatments at  $20^\circ\text{C}$  (see Experimental section), thus the following results are all referring to samples with equal initial microstructure properties.

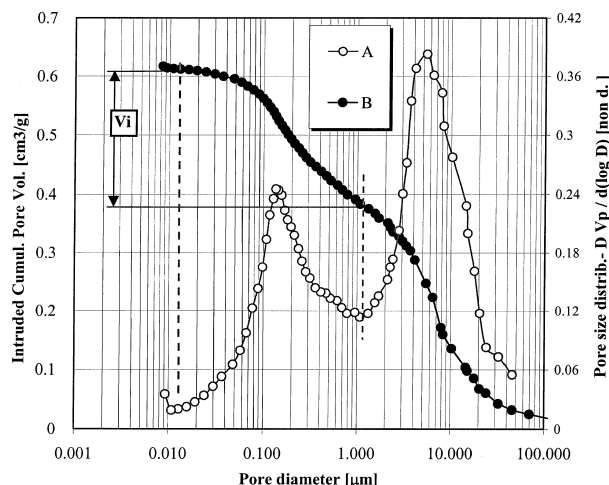


Fig. 2. Mercury porosimeter analysis of the  $\text{Ca}(\text{OH})_2$  powders: curve A, cumulative pore volume intruded; curve B, pore size distribution.  $V_i$  is the internal particles pore volume.

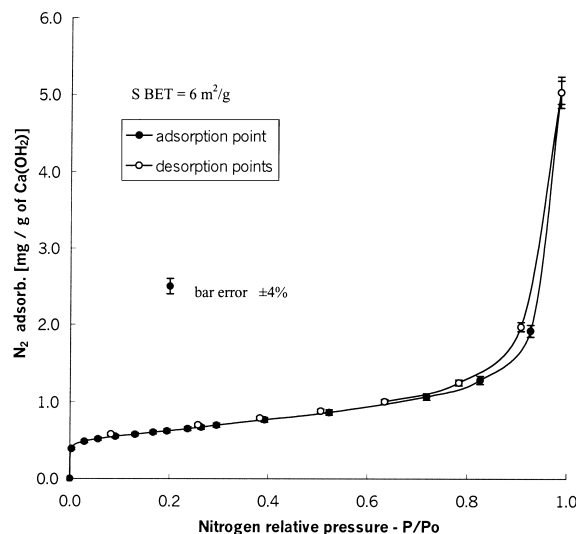


Fig. 3. Typical adsorption–desorption isotherms for the  $\text{Ca}(\text{OH})_2$  powders with  $\text{N}_2$  at  $78 \text{ K}$ .

To describe the reactivity of these powders with the gaseous carbon dioxide, let the experiments where the dry powders are reacting with  $\text{CO}_2$  (g) be named as GSC (gas–solid carbonation) tests, and the experiments where multilayers of water vapor have been adsorbed on the same powders, as WMC (carbonation with water multilayers).

Fig. 4 (curves a and b) describes the typical results from, respectively, GSC (curve a) and WMC (curve b) experiments. In both cases the carbon dioxide pressure was set to  $0.65 \text{ kPa}$ , but the process for the GSC run was carried out at the temperature of  $100^\circ\text{C}$ , while for the WMC the temperature was set at  $20^\circ\text{C}$ . Despite this difference, which should increase the reaction rate and the degree of carbonation of the GSC process, it can be

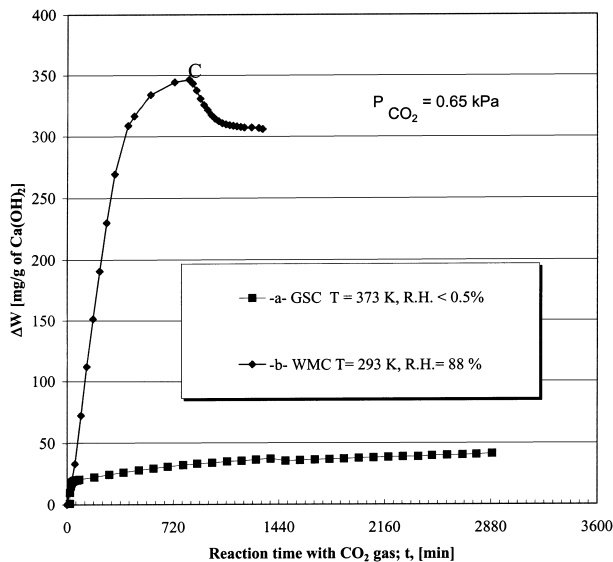


Fig. 4. Weight gain during the carbonation process: curve a, GSC reaction; curve b, WMC reaction.

observed that the WMC process is definitely more efficient in the  $\text{CO}_2$  uptake. The formed solid product is due in both cases to the  $\text{CaCO}_3$  phase, but with a degree of conversion of 10% for the GSC process and of 80% for the WMC one. Evidently, the adsorption of water vapor on the internal surface of the porous calcium hydroxide particles changes the reaction paths of the carbonation reaction.

In the area of cement chemistry it is well known<sup>17,18</sup> that the rate of carbonation is increasing with the presence of liquid water. Those results are in close agreement with the ones here and illustrate if the  $\text{H}_2\text{O}$  adsorbed multilayer films behave like liquid. To proceed to an interpretation of these new phenomena, it is interesting to consider the experimental data concerning the adsorption of water vapor on  $\text{Ca(OH)}_2$  and  $\text{CaCO}_3$  particles. Fig. 5 (curve a) shows the equilibrium adsorption isotherm of water vapor on the starting calcium hydroxides particles at  $20^\circ\text{C}$ . Curve b in the same figure is the equivalent equilibrium adsorption isotherm for water vapor on the calcium carbonate powders obtained from the complete carbonation of the hydroxide powders. To allow comparison of data the water adsorption amounts have been plotted per square meter of adsorbent. On the right axes of the same figure the number of adsorbed water vapor layers has been calculated, assuming that the average thickness of the water monolayer is  $3.1 \text{ \AA}$ . This value is calculated assuming for the adsorbed multilayer the same density of liquid water. As it is possible to observe for any relative pressure ranging between 0.1 and 1, the amount of water vapor adsorbed on the calcium hydroxide surfaces is always larger than that adsorbed on calcium carbonate. This result implies that, when calcium hydroxide particles equilibrated in water vapor are exposed to the presence of

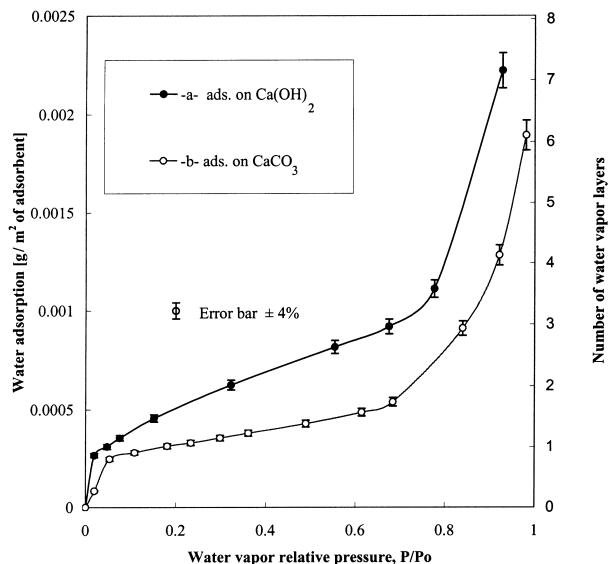
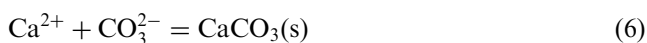
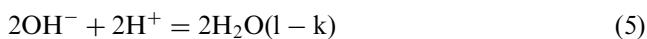
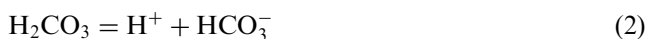


Fig. 5. Equilibrium adsorption isotherm of water vapour at 293 K: curve a,  $\text{Ca(OH)}_2$ ; curve b, on  $\text{CaCO}_3$ .

$\text{CO}_2(\text{g})$ , the amount of water vapor initially adsorbed tends to be reduced, because the formed calcium carbonate phase is more hydrophobic than calcium hydroxide.

On this evidence the WMC process can be described as formed by two stages: the carbonation of the calcium hydroxide particles and the vaporization of the water. The first step can be written as a sequence of the following ionic equations:



Symbols s, g and l – k are referring, respectively, to the solid, the gaseous and 2D liquid-like phases. Ion species are thought as solvated ion in the bidimensional liquid phase, and the dissociation of the carbonic acid is assumed to be irreversible.<sup>18</sup> Summation of Eqs. (1)–(6) leads to the global reaction:



The second step of the WMC process accounts for the water vaporization and it can be described through the equation:



where symbol  $v$  is referring to the vapor phase.

Experimental evidence that the above reported reactions are the main steps for the WMC processes is given by Fig. 4 (curve b). As is possible to observe, once that the sample reaches the maximum weight, it begins spontaneously to lose it (Fig. 4, point C in curve b). The slope of the curve plotting change in weight versus time can be understood through the joint global Eqs. (7) and (8). As soon as the  $\text{CO}_2$  (g) is introduced, the carbonation [eq. (7)] prevails since the surfaces are those formed by calcium hydroxide particles covered with water vapor. Then, when, the formation of the calcium carbonate phase is significant, [Eq. (8)] becomes progressively important up to point C where it becomes dominant.

Whether or not there is a critical amount of water adsorbed required to complete the carbonation with the WMC process is another question to be investigated.

Fig. 6 shows a set of WMC experiments carried out under the same experimental conditions of temperature ( $20^\circ\text{C}$ ) and carbon dioxide pressure (0.65 kPa) after having equilibrated the calcium hydroxide particles at different water vapor relative pressures. It is possible to observe that all kinetics follow initially an almost equal linear law followed by a plateau that occurs at reaction times which become shorter as the initial water vapor amount adsorbed decreases. In particular, if the amount of water vapor has been adsorbed below the relative pressure of 0.68, the effect of the water vapor in promoting the carbonation reactions seems to become negligible.

As shown by Fig. 5 (curve a) at the relative water vapor pressure of about 0.7, the water adsorption isotherm on

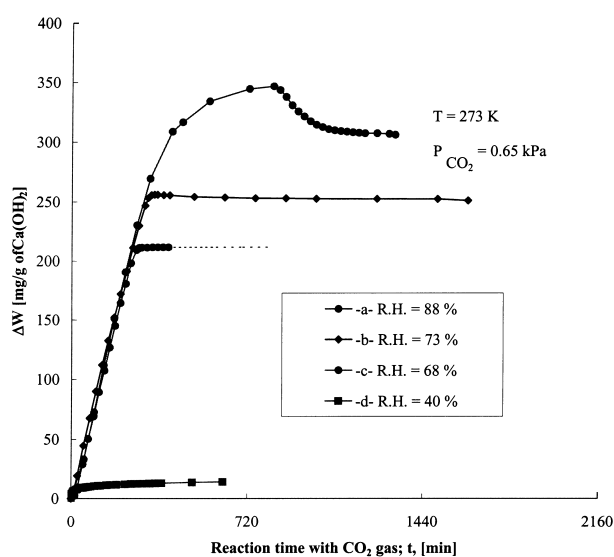


Fig. 6. Weight gain in  $\text{CO}_2$  (g)/ $\text{H}_2\text{O}$  (v) environment, at constant temperature and  $\text{CO}_2$  pressure, after equilibration at different water vapour pressure.

the calcium hydroxide surface increases its slope abruptly. It is possible that the water adsorption layers at this relative pressure became less bonded to the surfaces so that the reacting species are more mobile all along the interfacial reaction regions. When the amount of water adsorbed becomes less than that necessary to promote the surface mobility, the carbonation process should stop.

Fig. 7 is the experimental evidence of how the vaporization of water vapor according to Eq. (2) is really the rate limiting step for the carbonation to proceed. At some point B of the reaction branch where there was no weight gain, the partial pressure  $\text{CO}_2$  in the reaction chamber was raised keeping constant all other values. Then the  $\text{CO}_2$  pressure was lowered again to the previous value and the water vapor pressure was increased. No change in weight was observed with the introduction of  $\text{CO}_2$  but a rapid start of the reaction was recorded (see Fig. 7) when water vapor was introduced.

Taking into account the significant amount of calcium carbonate phase formed when the reaction stops, this experiment suggests also that the new calcium carbonate phase is not formed as a protective layer. In fact, with such a large amount of carbonate, the reaction would not be restored by the water vapor if the solid product phase covers all the reactants.

Fig. 8 shows a SEM picture of the final particles carbonated up to the 85% with the WMC process. As is possible to note, the macroscopic block-like structure of the initial particles (see Fig. 1) has not changed during the carbonation reaction. The final BET surface area for these particles has decreased to about  $3 \text{ m}^2/\text{g}$  compared with the initial value of  $6 \text{ m}^2/\text{g}$ . The approximated average grain size, evaluated through XRD techniques,<sup>19</sup> has

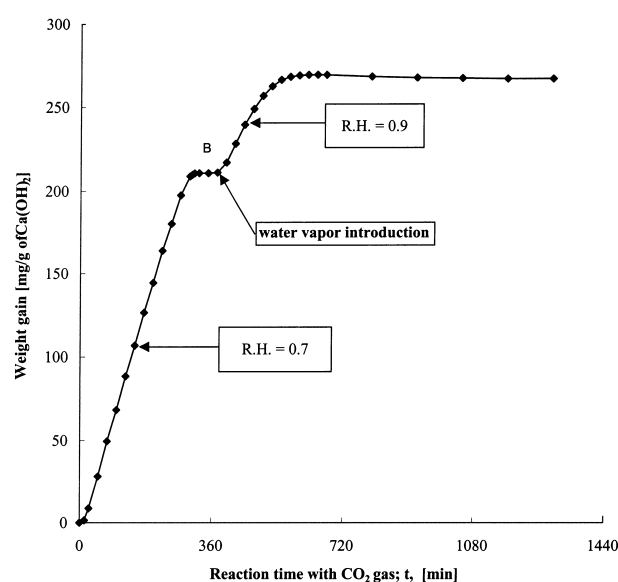


Fig. 7. Effect of water vapour introduction, the carbonation reaction restart when the relative partial pressure of  $\text{H}_2\text{O}$  (v) is increased.

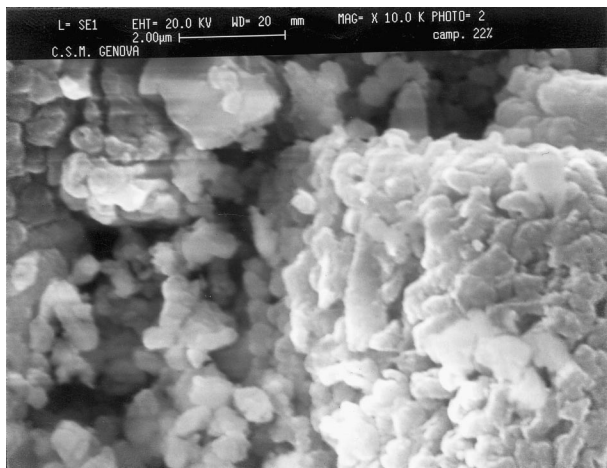


Fig. 8.  $\text{Ca}(\text{OH})_2$  carbonated with the WMC process up to 85% of conversion degree.

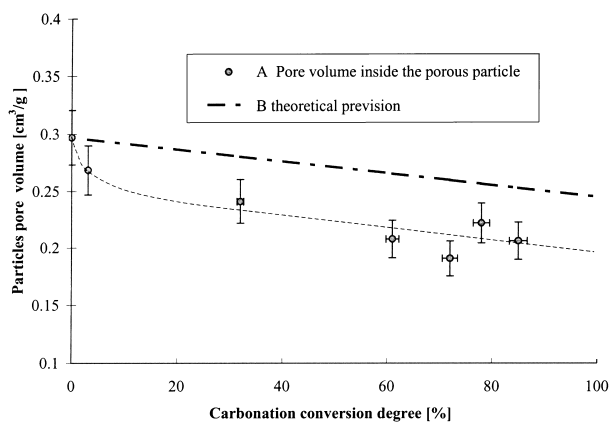


Fig. 9. Evolution of the internal particles porosity; porosity is referred to the initial weight of  $\text{Ca}(\text{OH})_2$ .

turned out to be 30 nm for  $\text{Ca}(\text{OH})_2$  and 50 nm for  $\text{CaCO}_3$ , in quite good agreement with the specific surface area measurement.

On the basis of these results the microstructure changes associated with the WMC process should occur inside the initial porous particles.

To test this possibility the evolution of the particle internal porosity has been measured as a function of the degree of carbonation. Fig. 9 (curve a) illustrates the results. In the same figure (line b) the theoretical decrease in porosity has been plotted, taking into account the difference in molar volume between calcium hydroxide and calcium carbonate phases.<sup>20</sup> If the calcium carbonate phase is formed inside the initial particles, the rate of porosity decrease should equal that predicted by the change in molar volume of the two solid phases. As is possible to observe, this prediction is experimentally meaningful if one neglects the initial porosity drop. The initial drop might reflect a collapse in the particle volume as has been observed also in other

cases<sup>13,21</sup> where a critical state of stress was reached inside the particles as a consequence of the reaction mechanism. Once that these stresses are released, a fairly stable porosity is left behind so that the carbonation, promoted by the water 2D liquid-like phase, can progress to the inside of the porous particles.

#### 4. Conclusions

1. Liquid-like water vapor adsorption layers catalyze the reaction between porous calcium hydroxides particles and carbon dioxide at the temperature of 20°C.
2. The formation of the new solid product phase enhances the evaporation of the adsorbed water so that the initial calcium hydroxide powders need be equilibrated with water vapor at a relative partial pressure greater and/or equal to 0.7 to promote significantly the catalytic reaction.
3. The new solid phase is formed by a non-protective layer of calcium carbonate that is entirely distributed inside the initial porous particles.

#### Acknowledgements

The authors are in debt to Professor A.W. Searcy for his very helpful contributions during the preparation of this work. Dr. D. Nardelli was helpful in collaborating with some of the experimental tests. This work was partially supported by the Italian MURST (40%) and by the University of Genoa.

#### References

1. Borgwart, R. H. and Bruce, K. R., Effect of the specific surface area on the reactivity of  $\text{CaO}$  with  $\text{SO}_2$ . *A. I. Ch. E. J.*, 1986, **32**, 239.
2. Collepardi, M., *Scienza e Tecnologia del Calcestruzzo*. Hoepli, Milan, 1991.
3. Laidler, K. J., *Chemical Kinetics*. McGraw-Hill, New York, 1965 (Chapter 5).
4. Gregg, S. J. and Sing, K. S. W., *Adsorption, Surface Area and Porosity*. Academic Press, New York, 1982, pp. 89–90.
5. Staudinger, G., Krammer, G. and Eckerstorfer, K., 90%  $\text{SO}_2$  removal with dry limestone. ARA process. In *Proceeding of  $\text{SO}_2$  Control Symposium*, New Orleans, LA, 8–11 May 1990.
6. Beruto, D. and Searcy, A. W., The liquid-like adsorption layers for removal of  $\text{SO}_2$  and/or  $\text{SO}_3$ , Invention Disclosure. L.B.L., Berkeley, 1994.
7. Beruto, D., Barco, L. and Searcy, A. W.,  $\text{CO}_2$ -catalyzed surface area and porosity changes in high-surface-area  $\text{CaO}$  aggregates. *J. Am. Ceram. Soc.*, 1984, **67**, 512–520.
8. Beruto, D., Botter, R. and Searcy, A. W.,  $\text{H}_2\text{O}$ -catalyzed sintering of  $\approx 2$ -nm-cross section particles of  $\text{MgO}$ . *J. Am. Ceram. Soc.*, 1987, **70**, 155–159.
9. Lee, H. E. D., Validity of using mercury porosimetry to characterize the pore structures of ceramic green compacts. *J. Am. Ceram. Soc.*, 1990, **73**, 2309–2315.

10. Gregg, S. J. and Sing, K. S. W., *Adsorption, Surface Area and Porosity*. Academic Press, New York, 1982.
11. Washburn, E. W., Note on a method of determining the distribution of pore size in a porous material. *Proc. Nat. Acad. Sci. U.S.A.*, 1921, 7, 115–16.
12. Brunauer, S., Deeming, L. S., Deeming, W. S. and Teller, E., Adsorption gases in multimolecular layers. *J. Am. Chem. Soc.*, 1938, 60, 309–319.
13. Beruto, D., Barco, L., Searcy, A. W. and Spinolo, G., Characterization of the porous CaO particles formed by decomposition of CaCO<sub>3</sub> and of Ca(OH)<sub>2</sub> in vacuum. *J. Am. Ceram. Soc.*, 1980, 63, 439–443.
14. Lippens, B. C. and De Boer, J. H., Studies of pore system in catalyst: V. *J. Catal.*, 1965, 4, 319–323.
15. Lippens, B. C. and De Boer, J. H., Studies on pore systems in catalysts. VII, Description of pore dimensions of carbon black by the *t*-method. *J. Catal.*, 1965, 4, 649–653.
16. Brunauer, S., Emmet, P. and Teller, E., Adsorption of gases in multimolecular layers. *J. Am. Chem. Soc.*, 1938, 60, 309–319.
17. Metha, P. K. and Monteiro, P. J. M., *Concrete Structure, Properties and Materials*. Prentice Hall Inc, Englewood Cliffs, NJ, 1993.
18. Moskvina, V., Ivanov, F., Alekseyev, S. and Guzeyev, E. *Concrete and Reinforced Concrete Deterioration and Protection*, ed. V. Moskvina. Mir Publisher, Moscow, 1980.
19. Klug, H. P. and Alexander, L. E., *X-ray Diffraction Procedures*. John Wiley and Sons, New York, 1954 (Chapter 9).
20. Beruto, D., Kim, M. G. and Searcy, A., Microstructure and reactivity of porous and ultrafine CaO particles with CO<sub>2</sub>. *High Temp. — High Press.*, 1988, 20, 25–30.
21. Beruto, D., Searcy, A. W. and Barco, L., Rearrangement of porous CaO aggregates during calcite decomposition in vacuum. *J. Am. Ceram. Soc.*, 1983, 66, 893–896.